Orbital energy of natural satellites converted into permanent power for spacecraft

J. Peláez *

January 14, 2008

1 Introduction

Some of the most startling discoveries about our solar system have been made in the outer planets. Jupiter predominates among these planets for many reasons. Just like the Sun, it has its own Jovian system. The study of this system has advanced our understanding of the broader solar system for nearly four centuries. Five NASA spacecraft flew past Jupiter in the past decades: Pioneer 10 and 11, Voyager 1 and 2 and Galileo.

However, outer planet exploration has always been handicapped by a scarcity of power. Solar panels become rapidly ineffective further from the Sun. The solar intensity at Jupiter, 5 AU distant from the Sun, is only one twenty-fifth of its value at Earth. As a consequence, energy is a *scarce commodity* in this kind of missions and the total energy which will be consumed by the spacecraft should be transported onboard.

To tackle this problem *Radioisotope Thermoelectric Generators* (RTG's) have been used as the source power in missions to the outer planets. These devices use thermocouples to convert into electrical energy the heat released by the natural decay of a strongly radioactive element (usually Pu - 238). RTG's exhibit three characteristics: *i)* the energy produced is expensive because the efficiency is low, ranging between 3% and 10% (at present, the estimated cost fluctuates from $40,000 to $400,000 per watt), *ii)* the potential risk is very high due to the management of very radiative substances and *iii)* the mass grows quickly with the energy produced. Table 1 summarizes power and mass of the RTG's used in several missions: the mass (in kg) is $\sim 20\%$ of the power (in watt).

Mission	Electrical W	Mass (kg)
Pionner 10	150	54.4
Voyager 1 y 2	470	117
Ulysses	290	55.5
Galileo	570	111
Cassini	800	168

Table 1: RTG's in past missions

These are reasons why NASA's Jupiter Icy Moon Orbiter (JIMO) mission investigated the use of a nuclear-powered craft. The spacecraft was to be propelled by a new kind of ion thruster (HiPEP), and powered by a small fission reactor. Such a mission to the Jovian Galilean moons, initially planned for 2015, was finally canceled in 2005.

*Prof of Aerospace Engineering, Technical University of Madrid (UPM), ETSI Aeronáuticos, Pz Cardenal Cisneros 3, E-28040, Madrid, Spain

2 Electrodynamic tethers

A conductive rod moving in a magnetic field $\vec{B}$ experiences a motional electric field given by

$$\vec{E} = \vec{v} \times \vec{B}$$

In the *vacuum*, a redistribution of surface charges takes place, leading to a vanishing electric field inside the rod. Thus, a steady state is reached with no motion of charged particles.

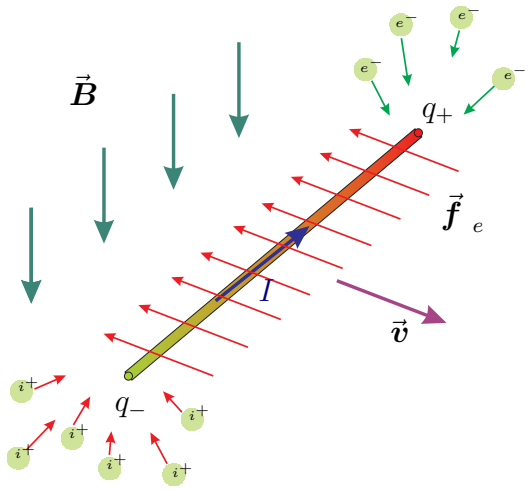

Figure 1: Conductive rod in a plasma environment moving in a magnetic field

If the rod is moving inside a *plasma environment*, this picture changes drastically. The plasma electrons are attracted by the anodic end of the rod and the ions by the cathodic end. Some of these charges are trapped by the rod and produce a current I which flows inside the conductive material. The amount of current can be increased with the help of plasma contactors placed at the rod ends. Such a rod is, basically, an electrodynamic tether (ET).

The interaction between the tether current I and the magnetic field $\vec{B}$ gives place to forces acting on the rod. They will break (or accelerate) its motion. Their resultant, $\vec{f}_e = L(\vec{I} \times \vec{B})$ is the *electrodynamic drag (or thrust)*. There are two basic regimes for an ET: the generator regime (drag) and the thruster regime (thrust).

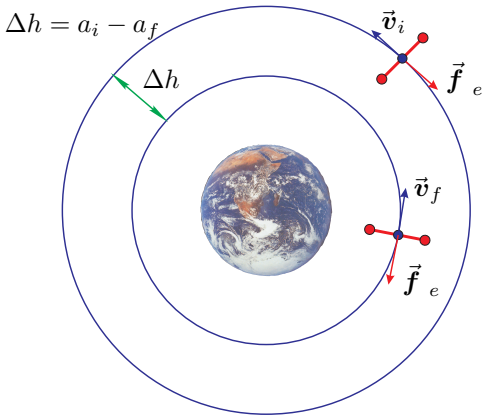

Figure 2: Deorbiting a satellite

Let m be the mass of a satellite orbiting around a planet. When it descends from an initial orbit of radius a_i to a final orbit of radius a_f the mechanical energy lost in the process is given by

$$\Delta E = \frac{m\mu}{2a_f}\frac{\Delta h}{a_i}$$

where μ is the gravitational constant of the planet. This approximated result assumes the orbital system behaves as a point mass.

ET's can deorbit satellites in different scenarios (see [1, 2, 3, 4]) due to their capacity to produce *electrodynamic drag* $\vec{f}_e$ when they operate in the generator regime. Such a *drag* brakes the spacecraft and provides the decay of the orbit. However, there are two essential requirements for the operation of an ET: 1) the magnetic field $\vec{B}$ and 2) the plasma environment. Both are absent at the Moon where an ET can not be operated. However, the Earth and other planets, Jupiter for example, are appropriated for the use of ET's.

3 Power generation

When using an ET the mechanical energy lost in the descent process is dissipated through different mechanisms (see [5]). Roughly speaking, one part is spent bringing electrons from infinity to the tether. More dissipation takes place at the cathodic contactor of the tether and through the ohmic losses along the wire. Finally, a part is dissipated in *any interposed load Z_T placed at the cathodic end of the tether.*

This last contribution is, in fact, **useful energy, i.e., energy that can be used onboard to perform some task** (charging batteries, moving electrical engines or feeding some electronic circuit). Depending on the tether configuration and the environment conditions this contribution could reach 40% of ΔE; values around 20% would be considered quite reasonable.

This property allows one to consider electrodynamic tethers as power sources, able to supply the whole system. In the generator regime they work converting mechanical energy into electrical energy and producing the required level of onboard energy; the bare tethers are particularly effective [6, 7]. As we show later on, in some missions a bare ET would provide much more energy than RTG's, enabling the utilization of more powerful instrumentation.

The essential idea of this work is to use an ET to obtain interesting amounts of power by deorbiting one of the Jupiter moonlets. Assume, for a moment, that the tether is joined to the moonlet with a cable; when the ET is switched on, *the electrodynamic drag will be transmitted to the moonlet through the tension of the cable* and the deorbiting process will start. The moonlet will be deorbited and therefore, its orbital radius will decrease as time goes on. This way the tether is able to recover a fraction

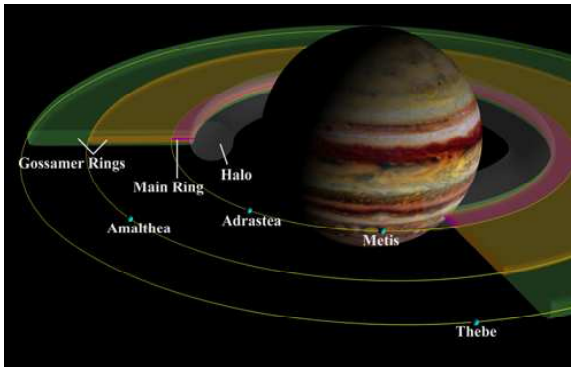

Figure 3: Jovian moonlets (from [14])

of the mechanical energy lost by the moonlet during the deorbiting process.

Two aspects should be underlined. First of all, the masses of the moonlets are larger than 10^{16} kg. For example, the mass of Amalthea is $m = 2.09 \times 10^{18}$ kg and its orbital radius is $a_i = 181,300$ km. If we deorbit Amalthea only 1 mm ($\Delta h = 1$ mm) a large amount of energy is obtained

$$\Delta E \approx 4 \times 10^{15}\text{J} \approx 1.1 \times 10^{9}\ \text{Kwh}$$

Thus, from a practical point of view, *the available energy is unbounded.*

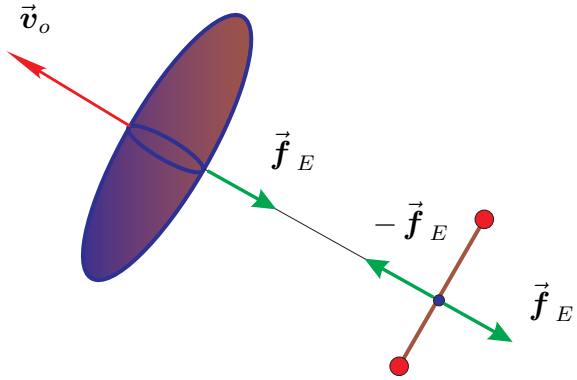

Figure 4: Deorbiting a Jovian moonlet

Second, the cable joining the S/C and the moonlet is not necessary; in effect, we can remove the cable if we place the S/C close enough to the moonlet. In such a case, the

gravitational force of the moonlet substitutes for the cable tension and the deorbiting process takes place in the same way.

If we place the probe in an equilibrium position relative to the system Jupiter-moonlet the ET will carry on deorbiting the moonlet indefinitely. Adjusting the tether length, diameter and material it is possible to obtain electrical power in a sustained way at Jupiter's neighborhood.

An ambitious attempt like this has, obviously, obstacles. Without a doubt, one of the greatest challenges is the extreme Jupiter radiation environment. This is a serious constraint that can be considered as a significant challenge for current or near-term developing technologies. Another problem is the uncertainty associated with the *electronic plasma density* in the neighborhoods of Jupiter; this parameter is important in the operation of any ET because the tether current strongly depends on it. In the following we will not focus on these challenges, however.

4 Dynamics

A detailed dynamical analysis can be found in [8, 9]. The main aspects will be described here from a global point of view.

There are three bodies involved in the problem: Jupiter, the inner moonlet and the S/C. Since all the moonlets have circular orbits around Jupiter with very small inclination it is appropriate to consider the problem as a generalization of the classical circular restricted three body problem (CRTBP), in a first approximation.

However, two significative differences should be emphasized: 1) electrodynamic forces are acting on the system and, 2) the attitude of the S/C should be considered since it plays an important role. Fig. 5

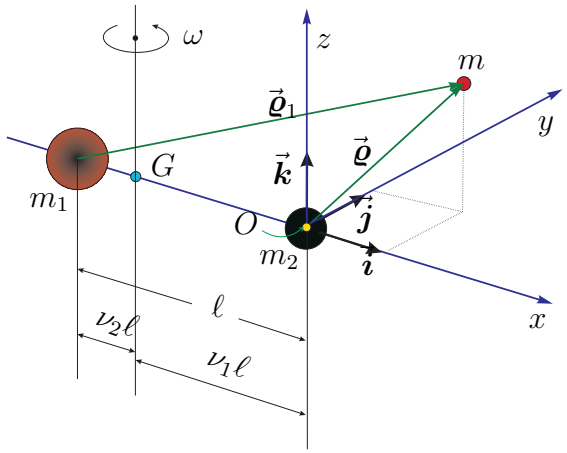

Figure 5: Reference frame

shows the *synodic frame* $Oxyz$ with origin at the center of mass of the Jovian moonlet, and where both primaries are at rest. The S/C must be placed in an equilibrium position relative to this frame.

Four main forces act on the system: the Jupiter gravity gradient, the Coriolis force, the gravitational attraction of the moonlet and the electrodynamic drag. Since the reduced mass ν of the moonlet is small the Hill approach provides an appropriated model to tackle the dynamic problem.

We will take a *bare* electrodynamic tether (BET) because is more effective collecting electrons. The electrodynamic forces play, obviously, an important role. They depend on the external fields (magnetic field and plasma environment) and on the tether design (material, cross section, length). Two non-dimensional parameters, (χ, ε) measure their influence:

$$\chi = \frac{I_m B_0 L}{m\ell\omega^2\nu^{\frac{1}{3}}}, \qquad \varepsilon = \frac{J_1 B_0}{I_s \omega^2} \tag{1}$$

Electrodynamic drag: the parameter χ is a measure of the electrodynamic drag. I_m is the averaged tether current, B_0 the magnetic field, L the tether length, m the mass of the S/C, ℓ the distance between

both primaries, ω the angular rate of the synodic frame and ν the reduced mass of the Jovian moonlet.

Lorentz torque: the parameter ε is a measure of the Lorentz torque at the center of mass of the S/C. I_s is the moment of inertia of the S/C relative to a straight line normal to the tether by the center of mass, and J_1 is the following integral

$$\frac{J_1}{\sigma E_m A_t L_*^2} = \int_0^{\ell_t} (\ell_t \cos^2\phi - \varsigma)\, i_e(\varsigma)\, d\varsigma \quad (2)$$

where ς is the non-dimensional distance from the upper tether end, $i_e(\varsigma)$ the current profile (non-dimensional), A_t the cross section of the tether, σ the electrical conductivity of the material, E_m the component along the tether of the induced electric field, ϕ the mass angle (see [10]), $\ell_t = L/L_*$ a non-dimensional tether length and L_* is a characteristic length typical from the bare ET's given by:

$$L_* = \frac{(m_e E_m)^{1/3}}{e\, 2^{7/3}} (3\pi \frac{\sigma h_t}{n_\infty})^{2/3}$$

which essentially depends on the electronic plasma density n_∞ of the environment and the transversal distance h_t; h_t is the radius for a round section, and the thickness for a tape (e electron charge, m_e electron mass).

A detailed analysis (see [8, 9]) provides two families of equilibrium positions of the S/C which depend on the value of χ. In the analysis the tether is self-balanced, that is, we select the mass angle ϕ in order to get a zero Lorentz torque (see [11, 12]). For both families the tether lies into the orbital plane of the moonlet. Fig. 6 shows the position of the center of mass for both families. We call *the main set* to the equilibrium positions close to the moonlet orbit (red line). A linear analysis shows stability when $\chi < 0.115$ for the main set; when $\chi > 0.115$ there are different instability regions and the tether can be operated in a reliable way by using a simple feedback control law (see [9]).

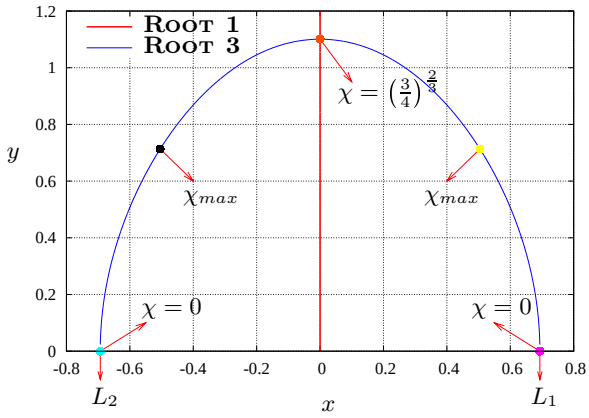

Figure 6: Equilibrium positions (x, y)

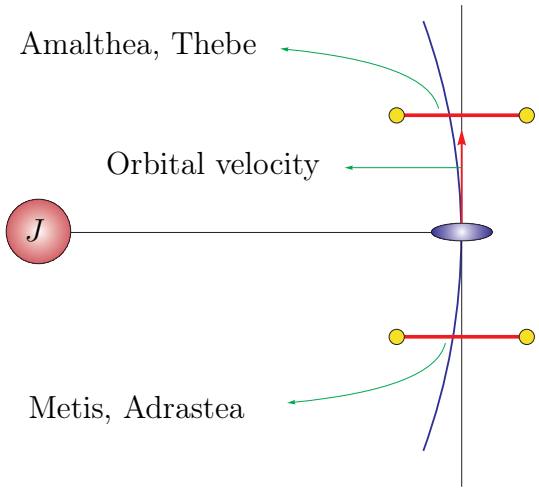

Figure 7: Relative position

Fig. 7 shows the relative position of the tethered system in the synodic frame. In two moonlets (Amalthea and Thebe) the BET is just in front of the moonlet. In the others (Adrastea and Metis) the BET is just behind the moonlet. This is due to the different position of the moonlets relative to the stationary Jovian orbit.

5 External fields

Magnetic field: in the neighborhoods of Jupiter the magnetic field is clearly dipolar and its polarity is just the opposite to the polarity of the geomagnetic field. As a consequence, it can be modeled as

$$\vec{\boldsymbol{B}}(\vec{\boldsymbol{r}}) = \mu_m \frac{R_J^3}{r^3}\big(\vec{\boldsymbol{u}}_m - 3(\vec{\boldsymbol{u}}_m \cdot \vec{\boldsymbol{u}}_r)\,\vec{\boldsymbol{u}}_r\big) \quad (3)$$

where $\mu_m = 4.27 \cdot 10^{-4}$ Teslas is the intensity of the dipole, $R_J = 71492$ km is the equatorial radius of Jupiter and $-\vec{\boldsymbol{u}}_m$ is a unit vector in the direction of the dipole. Since the tilt of the dipole is small, $\beta = 9.6°$, we assume a non-tilted dipole. This way the magnetic field, considering the Hill approximation, takes the value

$$\vec{\boldsymbol{B}} = B_0\,\vec{\boldsymbol{k}}, \qquad B_0 = \mu_m \frac{R_J^3}{\ell^3}$$

Inner plasmasphere: we follow the model of Divine & Garret (see [13]). When $R_J < r < 3.8R_J$ (the inner plasmasphere) the electronic plasma density, in m^{-3}, is given by

$$n_\infty = 4.65 \cdot 10^{-6} \exp\Big\{\frac{r_0}{r} - \big(\frac{r}{H_0} - 1\big)^2 (\lambda - \lambda_c)^2\Big\}$$

The parameters involved are

$$r_0 = 7.68R_J,\ H_0 = 1.0R_J,\ \lambda_c = 0.123\cos(l - l_0)$$

where l and λ are the longitude and latitude, in Jupiter System III (1965), respectively, and $l_0 = 21°$.

This model provides a quasi-constant value for the electronic plasma density at the orbits of the Jovian moonlets ($\lambda = 0°$). Fig. 8 shows the variations of n_∞ with l for the four satellites. The variation between the extreme values is lower than a 7% in all cases. This important fact permits to predict a small variation of the current collected in the BET without control.

We use another feature of the model of Divine & Garret: the most habitual ions in the region are: sulfur S^+ (about 70 %) and oxygen O^{++} (about 20 %).

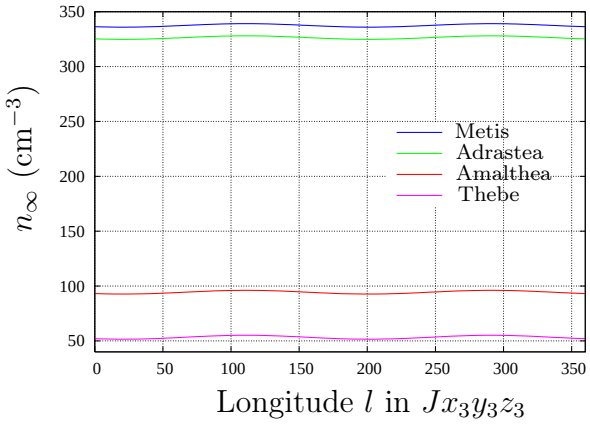

Figure 8: Electronic plasma density at the Jupiter moonlet orbits

6 Tether design

Fig. 9 shows an scheme of the BET. Let Z_T be the interposed load just placed at the cathodic end of the tether.

This load is essential and plays two complementary roles: 1) it is used to model the useful power obtained from the BET and 2) it permits the basic control of the system.

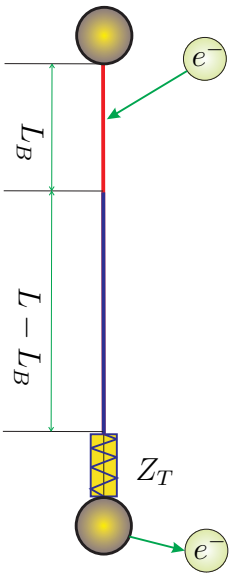

Figure 9: Tether scheme

The useful power that can be obtained from the tether is given by

$$W_u = I_C^2 Z_T$$

However, the main parameter in the tether design is the ratio W_u/m_T where m_T is the tether mass. It takes the value

$$\frac{W_u}{m_T} = \frac{\sigma E_m^2}{\rho_v} \cdot \Omega\, i_C^2(\ell_t, \Omega) \quad (4)$$

where ρ_v is the density of the material, $\Omega = Z_T/R_T$ is the non-dimensional form of the

interposed load Z_T (here, $R_T = L/(\sigma A_t)$ is the electrical resistance of the tether, I_C the current at the cathodic end).

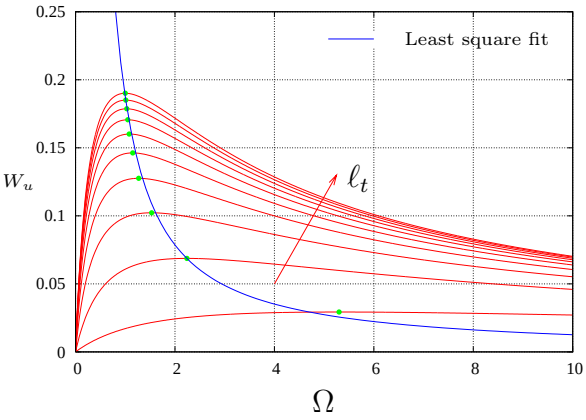

Figure 10: Useful power $W_u(\ell_t, \Omega)$; the picture shows the dependence on Ω for different values of $\ell_t = 0.5, 1.0, \ldots, 5$

In fact, assuming the BET is working in the OML regime, the electrodynamic performances of the tether are basically functions of only two parameters: the non-dimensional tether length ℓ_t and the non-dimensional interposed load Ω. Fig. 10 shows the dependence $W_u = W_u(\Omega)$ for different values of $\ell_t = 0.5, 1.0, \ldots, 5$. It is clear that there is a line of maxima $\tilde{\ell}_t = \ell_t(\Omega)\big|_{max}$. Along this line the tether performances are functions of only one parameter: the control parameter Ω.

Tether material: we select Aluminum since the ratio ρ_v/σ reaches a minimum value for it.

Selection of the Jovian moonlet: for any BET, the current collection is governed by the external fields. Particularly, the electronic density of the surrounding plasma n_∞ and the magnetic field (through the component of the electric field in the direction of the tether E_m). High values of these parameters make easy to operate the system because benefit the electron collection by the tether. As a consequence **we select Metis as the Jovian moonlet where the tether will be operated**.

Tether section: first of all, we will select the shape of the *tether cross section*: a tape of thickness h and width d_w. This rectangular section is more appropriate than a circular one because the value of L_* is lower for the same cross section; a lower value of L_* provides a higher value of ℓ_t and, in general, the electron collection will be benefitted. As a consequence, **tape is better than wire**. We must select the value of h as small as possible. At present, it is possible to make tapes as thin as $h = 0.1$ **mm**, and this will be the thickness of our tape. Perhaps in the near future thinner tapes can be constructed.

Useful energy: once the useful energy that the BET should provide is fixed, the tether length L, width d_w and mass m_T become functions of the control parameter Ω when we work on the line of maxima. Fig. 11 show this dependence for Metis and for a production of 500 watts of useful energy.

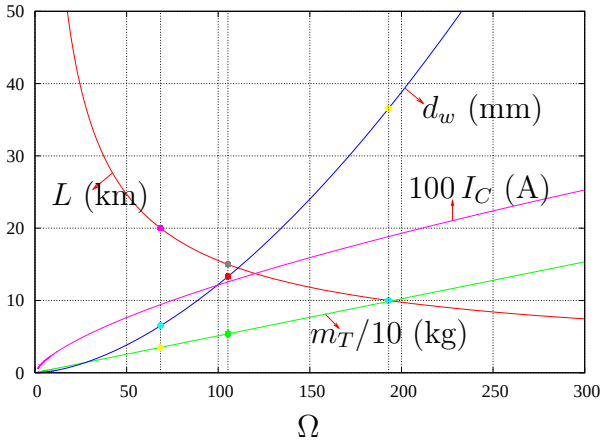

Figure 11: Optimum conditions at METIS ($h = 0.1$ mm, $W_u = 500$ w $\sim$ Galileo S/C)

Figure shows a wide range of **reasonable nominal values** which provide the desired useful energy.

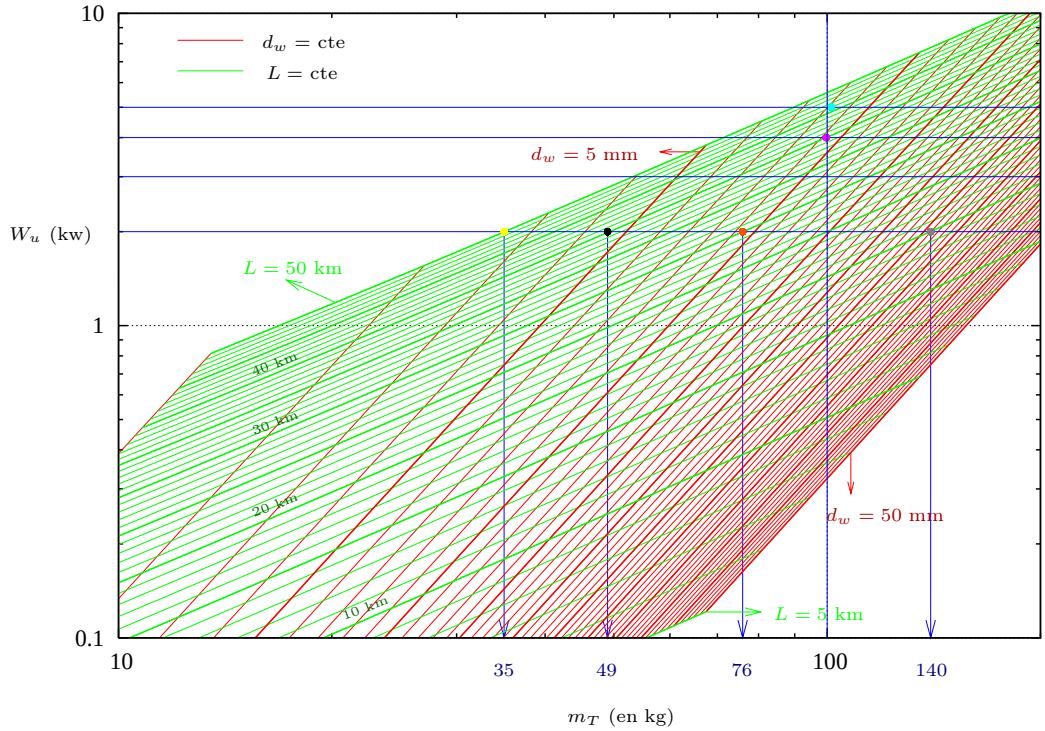

Figure 12: **Different optimized configurations in METIS** ($h = 0.1$ **mm**)

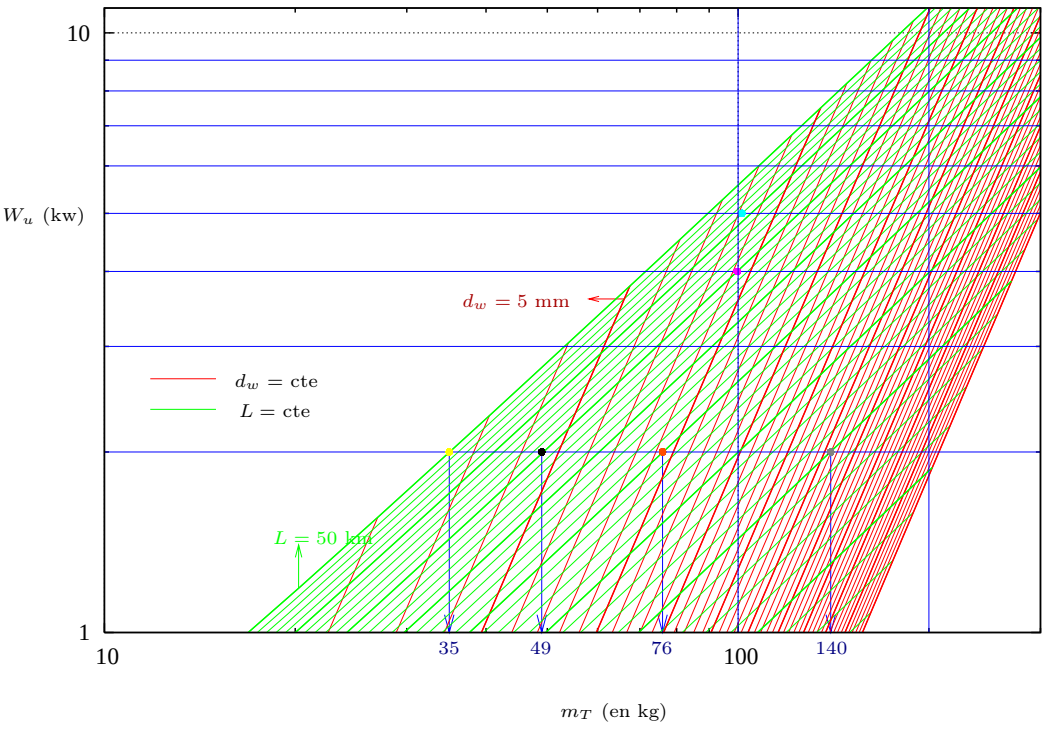

Figure 13: **Zoom of the previous figure focused on the more interesting region**

Obviously, the selection of one of these design should be made taking into account another factors not yet considered in the analysis. For example, the nominal value to be selected for Ω should involve a detailed study of the batteries charging process. These technological points should be clarified in the future, but for the moment they should be placed separately.

L (km)	d_w (mm)	m_T (kg)
50	2.7	35
40	4.7	49
30	9.5	76
20	26	140

Table 2: Some optimum configurations from figure 12 for $W_u = 2$ kw

7 Optimization

To understand more deeply the optimization process we constructed figure 12 which correspond to a tape operated in Metis and about 0.1 mm thick. In the abscissa-axis figure shows the tether mass m_T (in kg); in the ordinate-axis figure shows the useful energy provided by the tether (in kilowatts); in both axes we use a logarithmic scale. On the figure two families of curves have been drawn: the green lines show the variation of the useful power W_u with the tether mass m_T when the tether length L is fixed; along these lines the only parameter which changes is the tether width d_w. The red lines show the variation of the useful power W_u with the tether mass m_T when the tether width d_w is fixed; along these lines the only parameter which changes is the tether length L. For the red lines, the slope is larger than for the green lines, this explains why the useful energy is more sensitive to the variations of the tether length L than to the variations of the tether width d_w. Obviously, changing the tether length and width simultaneously is possible to increase W_u keeping the tether mass m_T constant.

Some important conclusions can be drawn from this figure. First of all, the BET provides more energy than the RTG's, for the same mass (around one order of magnitude more). For example, it is possible to obtain 500 w of useful power with a tether 17 km long and 10 mm width which weights 45.22 kg. The same level of energy produced by RTG's require much more mass: 111 kg in the case of the Galileo spacecraft. But there is a range of values of the useful energy that cannot be reached with RTG's because of the prohibitive mass required and, however, it can be reached with an BET. For example, a tether 30 km long and 9.5 mm width which weights 76 kg is able to produce 2000 w (see Table 2). To obtain this amount of energy with RTG's the mass required would be, probably, about hundreds of kg. Finally, we underline that with tether masses about 200 kg is possible to reach useful powers about 10 kw.

8 Conclusions

From our analysis some conclusions can be drawn; we comment them briefly in what follows.

1) Significant amounts of energy can be obtained by deorbiting any of the inner Jovian moonlets (Metis, Adrastea, Amalthea or Thebe). From a practical point of view Metis, the innermost moonlet, is the preferable to be deorbited with a bare, self-balanced, electrodynamic tether.

2) There exist equilibrium positions

where the tether could be operated appropriately; some of them are stable and other unstable. At first sight, the operation of the probe in an stable equilibrium position would be preferable; however, the probe would be operated in an unstable equilibrium position with the help of a feedback control law.

3) The appropriate parameter to establish a control strategy is a *variable interposed load* placed at the cathodic end of the tether. In that strategy the interposed load plays two simultaneous roles: *i)* it simulates the electrical resistance associated with the batteries of the S/C and *ii)* it controls the tether current acting as a potentiometer (in series with the batteries).

4) For the same mass the BET is able to produce more energy than traditional RTG's. In fact, by increasing the tether mass it would be possible to obtain much more energy (one order of magnitud more). Thus, the bare tether would open new prospects unattainable with RTG's.

5) The onboard energy provided by the bare tether is cheaper than the energy provided by RTG's.

There are many more points involved in a mission as the one proposed in these pages. For example, how to face the strong radiation environment in the neighborhood of Metis, or how to place the probe precisely in the equilibrium position where it should be operated. Some of these subjects will be studied in the near future.

References

[1] **G. Vannaroni, M. Dobrowolny and F. De Venuto**, "Deorbiting of LEO Satellites with Electrodynamic Tethers", *Proceedings Aerospace Sciences Meeting and Exhibit*, January, 2000.

[2] **J. Corsi & L. Iess**, "Stability and Control of Electrodynamic Tethers for De-orbiting Applications," *Acta Astronautica*, Vol. 48, No. 5-12, 2001, pp. 491–501.

[3] **L. Iess, C. Bruno, C. Ulivieri, et al.**, "Satellite de-orbiting by means of electrodynamic tethers - Part I: General concepts and requirements," *Acta Astronautica* , Vol. 50(7), 2002, pp. 399–406

[4] **L. Iess, C. Bruno, C. Ulivieri, et al.**, "Satellite de-orbiting by means of electrodynamic tethers - Part II: System configuration and performance," *Acta Astronautica* , Vol. 50(7), 2002, pp. 407–416

[5] **J. Peláez & M. Sanjurjo**, "Power generation using self-balanced electrodynamic tethers in debris mitigation scenarios" (Paper AAS07-196) of *The 2007 AAS/AIAA Space Flight Mechanics Meeting Sedona, Arizona, January 28 - February 1, 2007.*

[6] **J. R. Sanmartín, M. Martínez-Sánchez & E. Ahedo**, "Bare Wire Anodes for Electrodynamic Tether", *Journal of Propulsion and Power*, 9(0):352–320, 1993.

[7] **R. I. Samanta Roy, D. E. Hastings and E. Ahedo**, "Systems analysis of electrodynamic tethers," *Journal of Spacecraft and Rockets*, Vol. 29, 1992, pp. 415–424.

[8] **J. Peláez & D. J. Scheeres**, "A permanent tethered observatory at Jupiter. Dynamical analysis" (Paper AAS07-190) of *The 2007 AAS/AIAA Space Flight Mechanics Meeting Sedona, Arizona, January 28 - February 1, 2007.*

[9] **J. Peláez and D. J. Sheeres**, "On the control of a permanent tethered observatory at Jupiter", Paper AAS07-369 of the 2007 AAS/AIAA Astrodynamics Specialist Conference, Mackinac Island, Michigan, August 19-23, 2007

[10] **J. Peláez & M. Sanjurjo**, "Generator regime of self balanced electrodynamic bare tethers" *Journal of Spacecraft and Rockets*, Vol. 43, # 6, November-December 2006, pp. 1359-1369.

[11] **J. Peláez**, "Self balanced electrodynamic tethers," *Paper AIAA 2004-5309, The 2004 AAS/AIAA Astrodynamics Specialist Conference and Exhibit*, Providence, Rhode Island, USA, 16-19 August 2004.

[12] **J. Peláez, M. Sanjurjo & J. Fontdecaba**, "Satellite deorbiting using a self balanced electrodynamic tether," *Paper IAC-04-A.5.08, The 55th International Astronautical Congress*, Vancouver, Canada, October 2004.

[13] **N. Divine and H.B. Garrett**, "Charged Particle Distribution in Jupiter's Magnetosphere" *Journal of Geophysical Research*, Vol. 88 , No. A9, pp. 6889-6903, 1983.

[14] **Frank Bagenal, Timothy Dowling & William McKinnon Edts.**, "Jupiter, (The Planet, Satellites and Magnetosphere)" *Cambridge Planetary Science*, Cambridge University Press, Cambridge, UK, 2004